

Experimental demonstration of a leadless quantum-dot cellular automata cell

Islamshah Amlani,^{a)} Alexei O. Orlov, Ravi K. Kummamuru,^{b)} Gary H. Bernstein, Craig S. Lent, and Gregory L. Snider

Department of Electrical Engineering, University of Notre Dame, Notre Dame, Indiana 46556

(Received 7 April 2000; accepted for publication 31 May 2000)

We present the experimental characterization of a leadless (floating) double-dot system and a leadless quantum-dot cellular automata cell, where aluminum metal islands are connected to the environment only by capacitors. Here, single electron charge transfer can be accomplished only by the exchange of an electron between the dots. The charge state of the dots is monitored using metal islands configured as electrometers. We show improvements in the cell performance relative to leaded dots, and discuss possible implications of our leadless design to the quantum-dot cellular automata logic implementation. © 2000 American Institute of Physics. [S0003-6951(00)00731-2]

Recently, quantum-dot cellular automata (QCA) has received significant attention. In this transistorless approach to computation, logic levels are represented by the configurations of single electrons in coupled quantum-dot systems.¹⁻³ The simplest structure in this paradigm, a cell, consists of four dots located at the vertices of a square sharing two electrons between them. Due to electrostatic repulsion, the two electrons in each cell are forced to the opposite corners along one of the two diagonals. These diagonally aligned charge states are the ground states of the four-dot system, and are used to encode logic values “0” and “1.” Since the dot sizes can ultimately be as small as single molecules, the QCA architecture offers ultrahigh device density that is predicted to be both faster and more energy efficient than conventional complementary metal-oxide-semiconductor technology.

In the last few years, significant progress has been made toward the realization of basic QCA elements. So far, a fully functional QCA cell^{4,5} and a small chain of cells forming a binary wire⁶ have been demonstrated. A QCA-based digital logic gate that performs Boolean AND and OR operations was also demonstrated.⁷ Both theory and experiments suggest that these cells can achieve high operating frequencies.⁸

A common feature of all QCA implementations reported thus far is that the dots forming the cell were connected to source and drain leads that act as electron reservoirs. This was useful for the initial demonstration of QCA principles as it allowed tracing of single electron motion between dots and leads by monitoring the current through the source and drain. In this paper, we present a different implementation of QCA in which the dots are not connected to source and drain leads. Excluding these leads not only greatly simplifies device design, fabrication, and measurement, but also simplifies the interfacing of QCA arrays. These experiments demonstrate single electron transfer in a system completely galvanically decoupled from the environment.

The major difference between leaded and leadless dot

systems is that in leaded dots, electrons can be added or removed from the source and drain leads while in leadless dots, electrons can move only from one dot to another. This basic difference is evident in their charging diagrams, which identify stable charge regimes as a function of gate biases. In a leaded system, the charging diagram can be obtained simply by measuring conductance through the coupled dot system as a function of the two gate biases.⁹ In a leadless system, the subject of this paper, charge state of the dots can be determined only by using external electrometers.

We present two different devices to show (a) the externally measured charging diagram of a leadless double-dot system, and (b) QCA operation in a leadless cell. Both devices are realized on an oxidized Si surface using standard Al/AIO_x tunnel junction technology pioneered by Dolan.¹⁰ Aluminum islands and leads are patterned using electron beam lithography with a subsequent shadow evaporation process and an intermediate oxidation step. The islands in QCA measurements act as dots, and in this paper we will use these names interchangeably. The area of the fabricated tunnel junctions is typically 60×60 nm².

All measurements were carried out in a dilution refrigerator. The electron temperature of the device is 70 mK.⁶ The experiment was performed in a magnetic field of 1 T in order to suppress the superconductivity of aluminum at millikelvin temperatures. Standard ac lock-in techniques were used for all measurements. The typical capacitance of our tunnel junctions, extracted from the Coulomb gap of the electrometers, is approximately 320 aF.¹¹ Other lithographic and parasitic capacitances are obtained from the Coulomb blockade oscillations of electrometers as a function of various gate biases.

Our first device consists of two small isolated metal islands connected by a tunnel junction forming a double dot [Fig. 1(a)]. No electrons can be added to or removed from the double dot. However, electrons may be transferred from one dot to the other by applying biases to the gate electrodes. Each dot (labeled D₁ and D₂) is also capacitively coupled to an electrometer.¹² Figure 1(b) shows a measured charging diagram of the floating double dot. The grayscale map represents the experimentally observed potential profile of dot

^{a)}Present address: Islamshah Amlani, Motorola Labs, 2100 East Elliot Road, MD EL508, Tempe, AZ 85284.

^{b)}Electronic mail: ravi.k.kummamuru.1@nd.edu

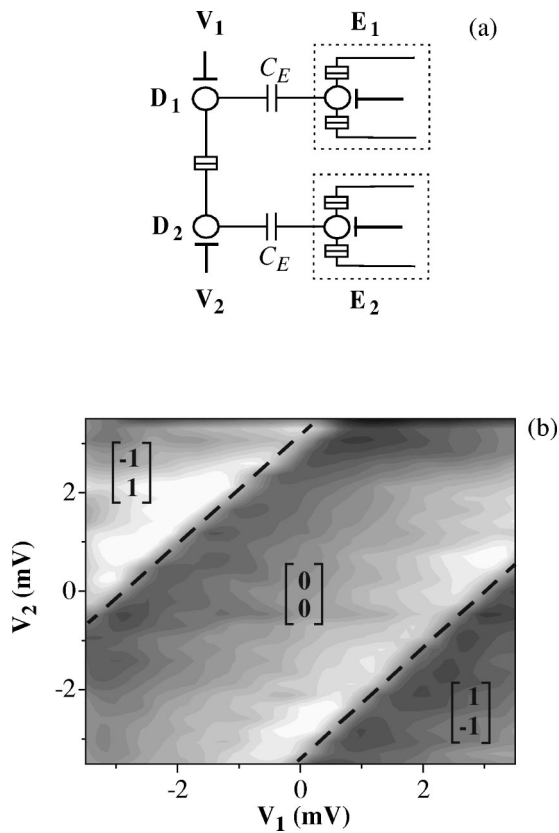


FIG. 1. (a) Schematic diagram of a leadless double-dot system. D_1 and D_2 are the two dots; E_1 and E_2 are the corresponding electrometers. (b) Charging diagram of a leadless double dot. The lighter shades represent higher dot potential. The numbers in the parentheses represent the charge configuration of the double dot.

D_1 .¹³ The potential of the other dot D_2 is similar but has the opposite phase. The dotted lines in Fig. 1(b) define the theoretically calculated borders between different charge states. Since the only possible source of electrons for one of the floating dots is the other dot, the only transitions possible are those when one dot loses an electron and the other acquires it.

We define the state with no applied bias as the neutral state with charge configuration (0,0) where there are no excess electrons on either of the dots (the charge configuration of the double dot represents the number of excess electrons in dots D_1 and D_2 , respectively). Let us consider transitions along the $V_1 = -V_2$ diagonal, which represents application of a differential bias to the dots D_1 and D_2 . As the differential bias is made sufficiently high to overcome Coulomb blockade in the double dot, one electron tunnels from D_2 to D_1 thus changing the charge configuration to (1, -1). If we further raise the bias applied to D_1 , one more electron will be lured onto D_1 from D_2 , changing the charge configuration to (2, -2) and so on.

Next, we consider our leadless QCA cell [Fig. 2(a)]. The cell consists of two capacitively coupled leadless (floating) double dots. The charge state of each of the four dots is monitored separately by the electrometers E_1 – E_4 . Figure 2(b) shows a scanning electron microscopy micrograph of a leadless QCA cell. Due to the symmetry of the structure, either of the double dots could be used as input or output, but for clarity, we will refer to the double dot on the left-hand side as the input double dot and the double dot on the right-

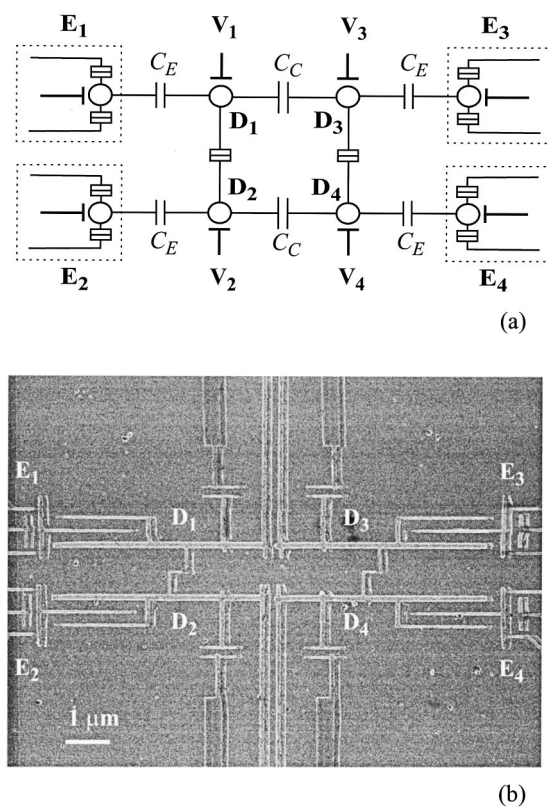


FIG. 2. (a) Schematic diagram of a leadless QCA cell. D_1 – D_4 are the four dots, and E_1 – E_4 are the corresponding electrometers. (b) SEM micrograph of the leadless QCA cell.

hand side as the output double dot. In the leadless implementation, QCA operation consists of causing an electron to switch in the input double dot D_1D_2 , which induces an electron to switch in the opposite direction in the output double dot D_3D_4 . The charge configuration of D_1D_2 changes from (0,0) \rightarrow (1, -1), which induces a change from (0,0) \rightarrow (-1,1) in D_3D_4 . This is actuated by applying a differential bias (with opposite polarities $V_1 = -V_2$) to the input double dot. Under the influence of the input bias, the potential of D_1 increases (the potential of D_2 decreases), until an electron tunnels from D_2 to D_1 producing an abrupt potential swing in the opposite direction. If the output double dot is biased anywhere on the boundary between two charge states [the dashed line in Fig. 1(a)], the potential perturbation produced by an electron exchange in the input double dot will cause an electron exchange in the opposite direction in the output double dot. This is markedly different from the case of QCA cell with leads, where many electron transitions are allowed and the desirable transition occurs when the bias point is set within a very small range of bias voltages.⁵

The results of the experiment are presented in Fig 3. The solid line in Fig. 3(a) shows the potential variation of D_1 (the change in potential of D_2 is similar but opposite in phase). The signal varies in a sawtooth manner, with the sharp transition corresponding to the transfer of a single electron in the input double dot from D_2 to D_1 . This transition causes the transfer of an electron in the opposite direction in the output double dot (from D_3 to D_4), as indicated by the solid line in Fig. 3(b). Thus, the data shown in Fig. 3 demonstrate QCA operation. The dashed lines in Figs. 3(a) and 3(b) show the

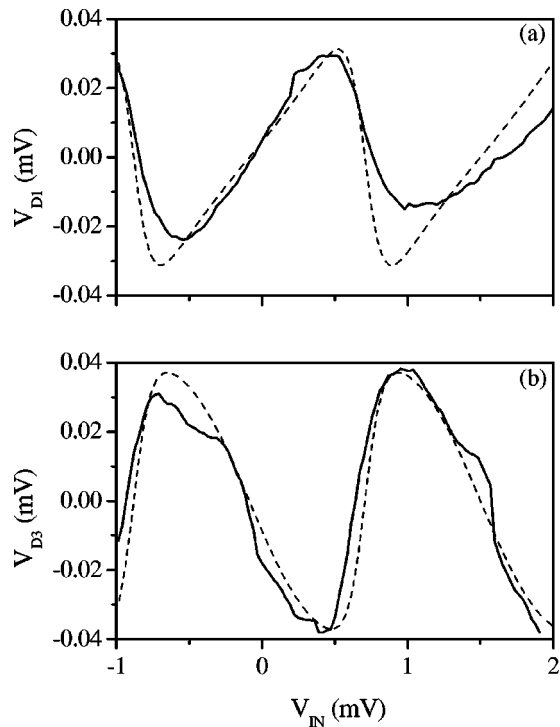


FIG. 3. QCA operation in a leadless cell. Measured (solid line) and calculated (dashed line) potential of (a) dot D_1 , (b) dot D_3 , with applied differential bias ($V_{in}=V_1=-V_2$).

simulated dot potentials for the two dots for a device temperature of 70 mK.

In Fig. 3 we notice that the potential swing in the output dot D_3 has a larger magnitude than that in the input dot D_1 . This effect arises due to thermal smearing. At 0 K the potential of the input dots, resulting from a linearly varying input bias, has a sawtooth shape. However, the potential on the output dots is affected only by the potential on the input dots and hence has a quasisquare wave shape⁴ with the same potential swing. At low temperature [$0 < kT \ll E_{\text{kink}}$ Ref. 14] thermal smearing causes a greater reduction in the potential swing in the input double dot than in the output double dot due to the difference in the shapes of the two wave forms. This results in larger amplitude of potential in the output dots than in the input dots. This effect was not observed in our previous experiments on QCA cells with leads.⁴⁻⁸ In the previous experiments, dots forming the cell were connected to source and drain leads by tunnel junctions, resulting in larger

dot capacitances due to the extra junctions and correspondingly smaller kink energy compared to the current device. Due to the smaller kink energy, the potential swing in the output dots was smaller than that in the input dots. The observation of larger amplitude in the output dot in the current device, in agreement with theory, confirms a more complete polarization change in the output dots than observed in previous experiments.

In conclusion, we have presented externally measured charging diagram of a leadless double dot and QCA operation in a leadless QCA cell. We have shown that the leadless dot design is simpler than the previous devices with leads and it can greatly simplify the fabrication of large QCA arrays. We have also shown that the leadless design results in better QCA performance in terms of output polarization change.

This research was supported in part by DARPA, ONR, and NSF. The authors are grateful to W. Porod and J. Merz for helpful discussions.

¹C. S. Lent and P. D. Tougaw, Proc. IEEE **85**, 541 (1997).

²C. S. Lent, P. D. Tougaw, and W. Porod, Appl. Phys. Lett. **62**, 714 (1993).

³C. S. Lent and P. D. Tougaw, J. Appl. Phys. **75**, 4077 (1994).

⁴A. O. Orlov, I. Amlani, G. H. Bernstein, C. S. Lent, and G. L. Snider, Science **277**, 928 (1997).

⁵I. Amlani, A. O. Orlov, G. L. Snider, C. S. Lent, and G. H. Bernstein, Appl. Phys. Lett. **72**, 2179 (1998).

⁶A. O. Orlov, I. Amlani, G. Toth, C. S. Lent, G. H. Bernstein, and G. L. Snider, Appl. Phys. Lett. **74**, 2875 (1999).

⁷I. Amlani, A. O. Orlov, G. Toth, G. H. Bernstein, C. S. Lent, and G. L. Snider, Science **284**, 289 (1999).

⁸A. O. Orlov, I. Amlani, G. Toth, C. S. Lent, G. H. Bernstein, and G. L. Snider, Appl. Phys. Lett. **73**, 2787 (1998).

⁹I. Amlani, A. O. Orlov, G. L. Snider, C. S. Lent, and G. H. Bernstein, Appl. Phys. Lett. **71**, 1730 (1997).

¹⁰T. A. Fulton and G. J. Dolan, Phys. Rev. Lett. **59**, 109 (1987).

¹¹Single Charge Tunneling, edited by H. Grabert and M. H. Devoret (Plenum, New York, 1992), Chaps. 1 and 2.

¹²G. L. Snider, A. O. Orlov, I. Amlani, X. Zuo, G. H. Bernstein, C. S. Lent, J. L. Merz, and W. Porod, J. Vac. Sci. Technol. A **17**, 1394 (1999).

¹³The technique we use to compensate for the effect of parasitic cross capacitances in the device also compensates for the monotonic change in potential on the dots. Therefore only the sawtooth pattern associated with the single-electron switching is seen.

¹⁴ E_{kink} is the characteristic kink energy of the device. We define the kink energy as the energy required to change the polarization of a cell from one binary state to the opposite. This energy, which depends on the coupling capacitance C_c and the dot capacitances, must be much greater than the thermal energy in order to observe a complete polarization change.